

Projections of Cold Air Outbreaks from Shared Socioeconomic Pathways in CMIP6 Earth System Models

Erik T Smith¹ and Scott C Sheridan²

¹Kent State University

²Kent State

November 21, 2022

Abstract

Historical and future simulated temperature data from five climate models in the Coupled Model Intercomparing Project Phase 6 (CMIP6) are used to understand how climate change might alter cold air outbreaks (CAOs) in the future. Three different Shared Socioeconomic Pathways (SSPs), SSP 1 – 2.6, SSP 2 – 4.5, and SSP 5 – 8.5 are examined to identify potential fluctuations in CAOs across the globe between 2015 and 2054. Though CAOs may remain persistent or even increase in some regions through 2040, all five climate models show CAOs disappearing by 2054. Climate models were able to accurately simulate the spatial distribution and trends of historical CAOs, but there were large errors in the simulated interannual frequency of CAOs in the North Atlantic and North Pacific. Fluctuations in complex processes, such as Atlantic Meridional Overturning Circulation, may be contributing to each model’s inability to simulate historical CAOs in these regions.

1 **Projections of Cold Air Outbreaks from Shared Socioeconomic Pathways in CMIP6 Earth**
2 **System Models**

3

4 Erik T. Smith*
5 Scott C. Sheridan

6

7

8 Kent State University; Department of Geography

9 *Corresponding Author Information:

10

11 Key Points:

- 12 1. Cold air outbreaks (CAOs) may largely disappear across the globe by 2054
13 2. CAOs may not decrease much for North America and Europe until closer to 2040
14 3. CMIP6 climate models struggle to simulate historical CAOs in several regions, like the
15 North Atlantic and North Pacific

16

17

18 **Abstract**

19 Historical and future simulated temperature data from five climate models in the Coupled
20 Model Intercomparing Project Phase 6 (CMIP6) are used to understand how climate change
21 might alter cold air outbreaks (CAOs) in the future. Three different Shared Socioeconomic
22 Pathways (SSPs), SSP 1 – 2.6, SSP 2 – 4.5, and SSP 5 – 8.5 are examined to identify potential
23 fluctuations in CAOs across the globe between 2015 and 2054. Though CAOs may remain
24 persistent or even increase in some regions through 2040, all five climate models show CAOs
25 disappearing by 2054. Climate models were able to accurately simulate the spatial distribution
26 and trends of historical CAOs, but there were large errors in the simulated interannual
27 frequency of CAOs in the North Atlantic and North Pacific. Fluctuations in complex processes,
28 such as Atlantic Meridional Overturning Circulation, may be contributing to each model's
29 inability to simulate historical CAOs in these regions.

30

31 **Plain Language Summary**

32 Cold air outbreaks (CAOs) are extreme events that can have large, negative impacts on society.
33 Because of these impacts it is important to understand how climate change might alter CAOs in
34 the future. Three future scenarios from five different climate models are examined to see
35 where CAOs might change the most between 2015 and 2054. While changes in CAOs may be
36 small for some regions through 2040, all the climate models show CAOs disappearing by 2054.
37 Where the climate models did a good job simulating historical CAOs, like in North America, we
38 have confidence that future projections are relatively accurate. Where the models did poorly at
39 simulating historical CAOs, like the North Atlantic and North Pacific, we have less confidence in
40 future projections. More work needs to be done to understand the complex processes that
41 lead to these errors.

42

43 **Keywords:** Cold air outbreaks, extreme cold events, climate modeling, ERA5, CMIP6, shared
44 socioeconomic pathways

45 **1. Introduction**

46 Cold Air Outbreaks (CAO) are extreme events that can negatively impact multiple facets of
47 society. Though infrequent, extreme weather events cause significantly more damage than
48 non-extreme events (Bell et al., 2018; Schewe et al., 2019). CAOs have been shown to increase
49 the risk of human mortality (Smith & Sheridan, 2019), cause agricultural production losses (Lesk
50 et al., 2016), and cause widespread power outages from increased energy consumption (Y. Kim
51 & Lee, 2019; Klinger et al., 2014). Because of the large impacts on society, accurately projecting
52 how extremes like CAOs will change under future warming scenarios is a critical step in
53 developing a more resilient society.

54

55 Climate models, which are derived from substantiated physical principles of the earth system
56 process, are the best tool we have for predicting changes in CAOs (Flato, 2011; Räisänen,
57 2007; Randall et al., 2007). Climate models use dynamical and statistical calculations to
58 represent earth's climate system and propagate the current atmospheric state forward in time
59 (Collins et al., 2013; Randall et al., 2007; Richardson, 2007). The accuracy of future projections
60 depends on the data used to initialize the climate model, thus small inaccuracies are
61 exacerbated through time, leading to increased error with longer range projections (Polkova et
62 al., 2019). With no way to evaluate future projections from climate models, the ability of a
63 climate model to represent future climates must be assessed by comparing simulations of
64 historical climates with observations or reanalysis datasets (Edwards, 2011). While observations
65 are point based, atmospheric reanalysis datasets are a gridded historical dataset of global
66 atmospheric circulation that use weather models to reanalyze assimilated observations over
67 much shorter timescales than climate models (Dee et al., 2011). Because reanalysis datasets are
68 gridded, they provide an easier comparison with climate model output. They also allow
69 comparisons in data sparse regions like the Arctic and across oceans.

70

71 The Coupled Model Intercomparison Project (CMIP) has become the foundation for numerous
72 climate assessments (IPCC, 2013). CMIP uses multiple climate models from modelling centers

73 around the world to better understand past climates and future changes (Eyring et al., 2016).
74 Phase 6 of CMIP (CMIP6) aims to make the multi-model output publicly available and more
75 user-friendly by standardizing the format. New to CMIP6 is the Scenario Model Intercomparison
76 Project (ScenarioMIP), which integrates inputs from both the climate science and integrated
77 assessment modelling communities to create future modeling scenarios (Eyring et al., 2016;
78 O'Neill et al., 2016; Tebaldi et al., 2020). These new scenarios, called Shared Socioeconomic
79 Pathways (SSPs), combine pathways of future radiative forcing with alternative pathways of
80 socioeconomic development to characterize the range of uncertainty in climate adaptation and
81 mitigation efforts (O'Neill et al., 2014). Global energy systems, which are the leading
82 contributor to carbon emissions, are particularly vulnerable to climate changes, yet
83 developments are limited by political and social acceptance (Bauer et al., 2017). The addition of
84 SSPs in CMIP6 is an essential step in determining how carbon emissions may fluctuate with
85 changes in global energy systems (Davis et al., 2018; X. Liu et al., 2019).

86

87 Though we cannot be certain if modeled changes in CAOs will be realized, we can get a good
88 idea if models are on the right track based on how models simulate historical climates (Jeuken
89 et al., 1996; Han-Li Liu et al., 2018). While many studies have examined projected changes in air
90 temperature (Almazroui et al., 2020; Friedrich et al., 2016; Jones et al., 2013; Kumar et al.,
91 2013; Tokarska et al., 2020), only a few studies have explicitly investigated changes in CAOs
92 (Kolstad & Bracegirdle, 2008; Vavrus et al., 2006). These studies showed that while CAOs have
93 decreased across much of the globe in recent decades, there was also an increase in some
94 regions (J. L. Cohen et al., 2012; Smith & Sheridan, 2020). While this increase in CAOs may
95 continue over the next few decades for some regions (Kolstad & Bracegirdle, 2008; Vavrus et
96 al., 2006), most places will likely experience a large decrease in CAOs throughout the 21st
97 century (Ayarzagüena & Screen, 2016; Vavrus et al., 2006; Zahn & von Storch, 2010).

98

99 This study uses climate model output from CMIP6 to better understand how the frequency of
100 CAOs may change across the globe between 2015 and 2054. Historical climate model

101 simulations from 1979 – 2014 are examined to determine how well five different climate
102 models reproduce the spatial and temporal distribution of CAOs. Three different SSPs are
103 examined to determine a range of potential fluctuations in CAOs between 2015 and 2054.
104 These findings have the potential to mitigate damages and future energy system vulnerabilities
105 by quantifying regional changes in CAOs.

106

107 **2. Data and Methods**

108 The global CAO dataset from Smith (2020) and CAO regions created by Smith & Sheridan (2020)
109 were used to compare historical CMIP6 CAO simulations with actual CAOs. This CAO dataset
110 was created from daily mean T2m from the ERA5 reanalysis dataset from the European Center
111 for Medium-Range Weather Forecasts (ECMWF; from
112 <https://cds.climate.copernicus.eu/cdsapp#!/home>; Copernicus Climate Change Service) at a 1°
113 spatial resolution from 1979 – 2014. CAOs were quantified using a set of criteria concerning
114 intensity, duration, and spatial extent of the extreme cold airmass, where the daily mean T2m
115 was required to be below the 2.5th percentile, based on the 1981 – 2010 climate normal period,
116 for at least 5 consecutive days for a contiguous area of at least 1,000,000 km² (Smith &
117 Sheridan, 2020). The use of a percentile threshold limits the impact of the skewness of the data
118 on the spatial distribution of CAOs. Future simulations of CAOs use the percentile thresholds
119 from the 1981 – 2010 climate normal period. CAO regions were used to simplify the analysis
120 from thousands of grid points to 10 regions with similar CAO characteristics and CAO trends
121 (Smith & Sheridan, 2020).

122

123 As CMIP6 is still in progress, output from all models is not yet available. Historical and projected
124 daily mean two-meter temperature (T2m) data were acquired from the same variant, r1i1p1f1,
125 of five Earth System Models: CESM2, CESM2-WACCM, MPI-ESM1-2-HR, MRI-ESM2-0, and
126 CanESM5 (Danabasoglu et al., 2020; Gutjahr et al. 2019; Swart et al., 2019; Yukimoto et al.,
127 2019). Three different shared socioeconomic pathways (SSPs), SSP1, SSP2, and SSP5 are
128 integrated with three different forcing pathways stabilizing at 2.6 W m⁻², 4.5 W m⁻², 8.5 W m⁻²

129 to create three scenarios of future climate and societal change (O'Neill et al., 2014). From each
130 of the five climate models, these integrated scenarios, denoted as SSP1-2.6 (SSP126), SSP2-4.5
131 (SSP245), and SSP5-8.5 (SSP585), were used to explore a range of potential changes in CAOs
132 across the globe. Data from the CMIP6 archive is publicly available from the Earth System Grid
133 Federation (ESGF; <https://esgf-node.llnl.gov/search/cmip6/>). To maintain consistency with the
134 time period used in Smith & Sheridan (2020) and because CMIP6 historical output ends in 2014,
135 historical T2m was acquired for 1979 – 2014 while projected T2m was acquired for 2015 –
136 2054. These five models allow for an in-depth analysis of both historical climate simulations and
137 future projections of CAOs. The T2m for each climate model was regridded to a 1° x 1°
138 resolution using a bilinear interpolation to match the resolution of the ERA5 derived CAO
139 dataset. Because bilinear interpolation creates a quadratic sample by linearly interpolating the
140 data in two different directions, it is generally better at rescaling data than a linear
141 interpolation (Wang et al., 2016).

142

143 Trends in the annual number of CAO days, derived from historical T2m climate model output,
144 were calculated and compared with the observed trends. This is used to determine if each
145 climate model is able to accurately simulate spatial and temporal fluctuations in CAOs. As
146 outlined by Smith & Sheridan (2020), trends for the Southern Hemisphere (SH) were calculated
147 for 36 winter seasons (January 1 – December 31) while trends in the Northern Hemisphere (NH)
148 were calculated for 35 winter seasons (July 1 – June 30). Due to the limited sample size (35 in
149 NH and 36 in SH), a Theil-Sen slope estimation was calculated from 1000 bootstrapped samples
150 and statistical significance determined from the confidence intervals produced from the
151 bootstrapped samples. Moreover, a false detection rate was used to limit the false significance
152 of the spatiotemporal relationships of the gridded data (Wilks, 2016).

153

154 Because of inherent errors in climate model simulations, various statistical or dynamical
155 techniques are often used to reduce biases (Maraun, 2016). However, many of these methods
156 can mask the uncertainty in projections by altering simulations without providing a physical

157 mechanism to explain why the corrections reduce the bias (Ehret et al., 2012). Climate
158 projections based on an ensemble of several models increase the reliability and consistency of
159 independent projections while maintaining transparency of systematic model errors (Tebaldi et
160 al., 2020; Yun et al., 2003). For this reason, the mean of the five climate models is used as an
161 ensemble for both historical simulations and each SSP to provide the least biased estimate of
162 future changes in CAOs.

163

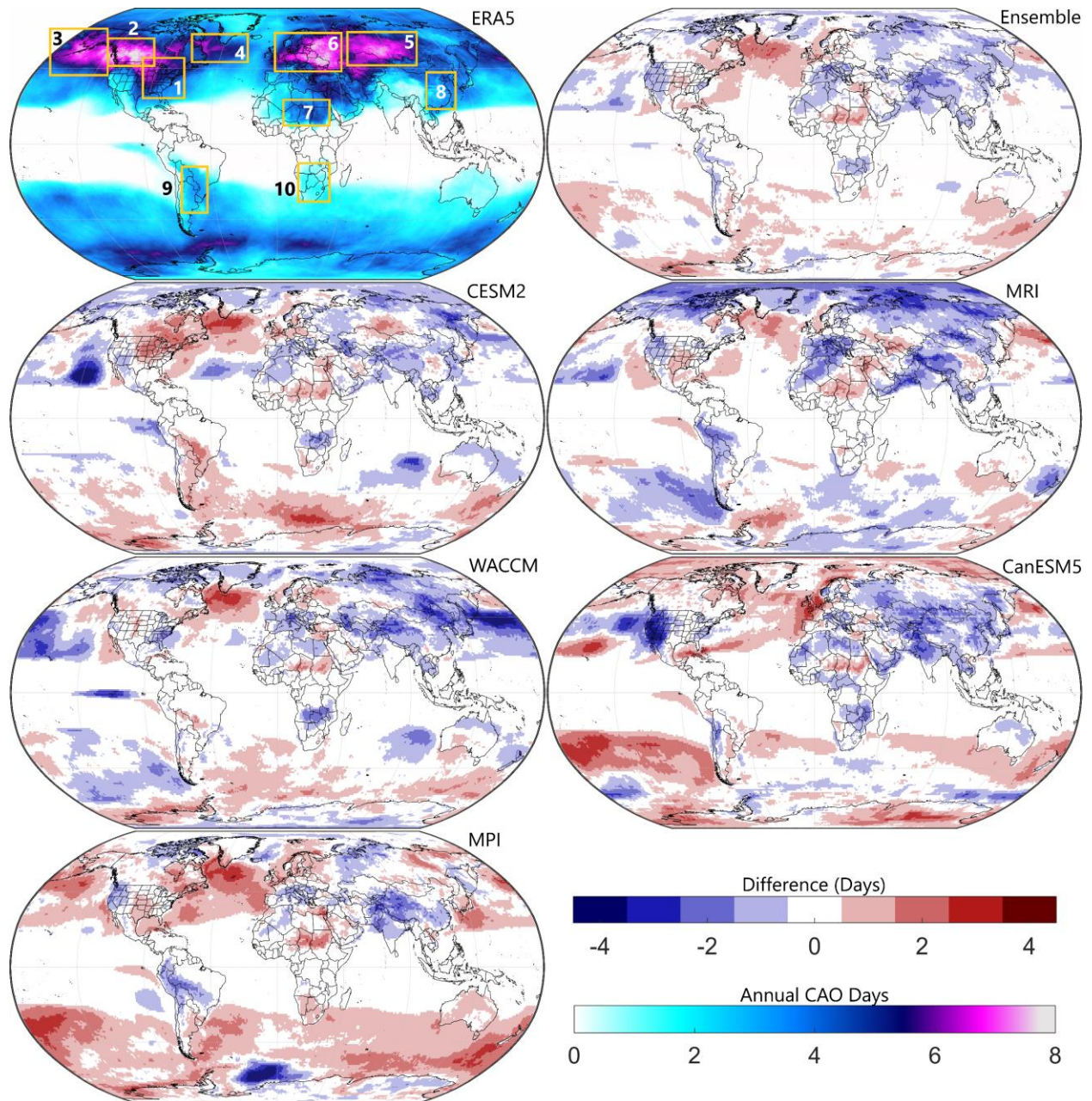
164 **3. Results**

165 **3.1. Historical Simulations of CAOs**

166 From 1979 – 2014, CAOs occurred most frequently across North America and Eurasia. Each of
167 the five climate models were able to reproduce the same general spatial distribution of CAOs as
168 observed with the ERA5, however, each model had a warm bias in the North Atlantic, with the
169 CESM2, WACCM, and MPI having the largest bias (Figure 1). This bias can likely be attributed to
170 how each climate model handles the Atlantic Meridional Overturning Circulation (AMOC; Gent,
171 2018) or air-sea interactions from fluctuations in Arctic sea ice (Kolstad & Bracegirdle, 2008).
172 Climate model simulations have been shown to underestimate the weakening of the AMOC (Hu
173 et al., 2013; Meehl et al., 2020), which favors more CAOs in the North Atlantic. This may
174 account for the simulation of too few CAOs early in the historical period (R4; Figure A1). The
175 CanESM5 has a cold bias across the western United States and like the MPI, a warm bias across
176 the oceans which is largest in the Southern Pacific. Conversely, the MRI has a large cold bias in
177 the Northern Hemisphere (NH), particularly across the Arctic.

178

179 Spatial and temporal similarity were calculated to determine which climate model most
180 accurately simulated the spatial distribution and annual frequency of CAOs for each region
181 (Table 2). While each model was able to simulate the general spatial distribution of CAOs, some
182 regions were better modeled than others (SS; Table 2). Moreover, there were large
183 discrepancies between the time series of mean regional annual CAO days simulated by the
184 climate models and



185

186 *Figure 1: Observed annual cold air outbreak (CAO) days from 1979 – 2014 (ERA5) and the difference between the simulated*
 187 *annual CAO days for the five CMIP6 climate models (CESM2, WACCM, MPI, MRI, and CanESM5) and the ensemble. Regions are*
 188 *denoted with bounding boxes in the ERA5 figure (Smith and Sheridan, 2020).*

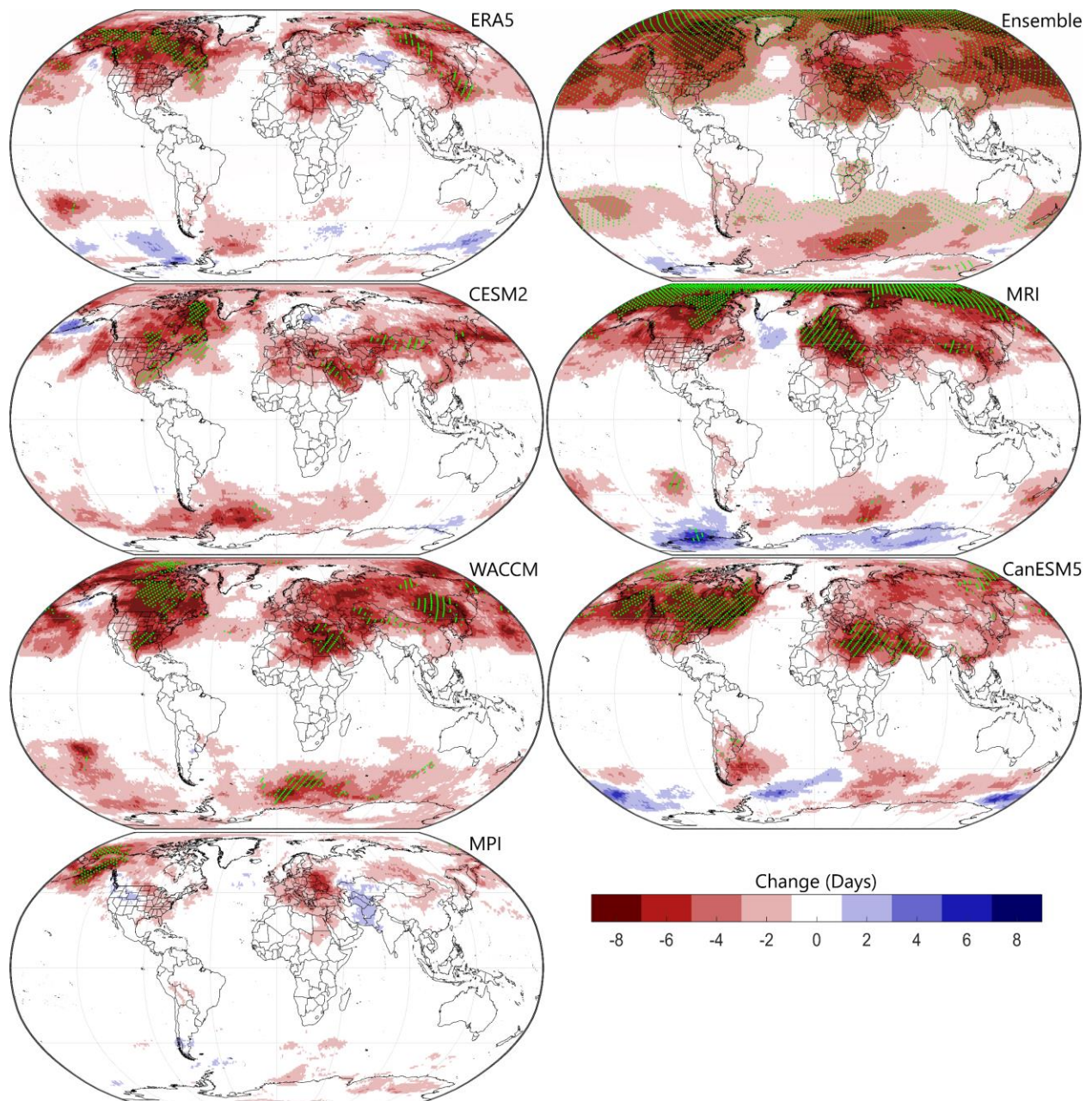
189 the mean regional annual CAO days from the ERA5 (mean absolute error; MAE; Table2). The
 190 CESM2 and MPI had a large warm bias across multiple regions and the largest total error in the
 191 SS of annual CAO days. The WACCM (full name: CESM2-WACCM), an extension of CESM2 that
 192 models the entire atmosphere (Liu et al., 2010), had less overall bias in SS than the CESM2,
 193 followed by the CanESM5 and the MRI. The MRI had the lowest MAE with North America (R1

194 and R2) while the MPI and WACCM had the lowest MAE in Eurasia. In nearly every region, the
 195 model ensemble reduces the errors in spatial similarity (SS) and temporal similarity (MAE).

196 *Table 1: Climate model spatial (SS) and temporal (MAE) historical simulation accuracy (1979-2014). Spatial similarity (SS) -*
 197 *difference between regional mean annual CAO days and the observed annual mean CAO days from the ERA5. The mean*
 198 *absolute error (MAE) is calculated for the annual number of CAO days per region in the historical climate model simulations and*
 199 *the observed (ERA5). Red/blue SS shows where the mean annual CAO days is less than/more than the ERA5. A red/yellow MAE*
 200 *shows where the MAE is large/small. Color intensity of the MAE is relative to the region. Total error is the sum of the absolute*
 201 *values of each column.*

Region	CESM2		WACCM		MPI		MRI		CanESM5		Ensemble	
	SS	MAE	SS	MAE	SS	MAE	SS	MAE	SS	MAE	SS	MAE
R1	-1.0	3.7	0.2	4.1	-0.5	3.9	-0.2	3.2	0.2	3.9	-0.3	2.8
R2	-0.2	5.2	-0.2	6.0	0.0	6.3	0.2	4.6	0.0	4.7	0.0	4.2
R3	0.3	5.4	0.1	5.5	-1.2	5.0	0.2	5.3	-0.4	5.7	-0.2	4.3
R4	-1.7	4.3	-1.6	5.0	-1.9	5.0	-1.0	5.6	-1.0	4.1	-1.4	4.2
R5	-0.6	5.5	0.4	4.9	0.1	5.1	0.9	5.6	0.8	6.7	0.3	4.4
R6	0.2	5.4	0.0	4.7	-0.3	4.5	0.5	5.8	-0.1	5.5	0.1	3.9
R7	-0.8	4.6	-0.4	4.8	-0.9	4.0	-1.0	3.3	-0.5	3.2	-0.7	3.3
R8	0.0	3.6	0.6	3.6	0.6	3.4	-0.3	2.9	0.8	3.9	0.3	2.9
R9	-1.0	2.6	-0.2	2.6	0.3	2.5	0.6	3.3	-0.3	2.2	-0.1	2.2
R10	-0.1	1.5	0.2	2.0	-0.6	1.6	0.1	1.5	0.3	1.7	0.0	1.3
Total Error	5.7	42.0	4.0	43.3	6.5	41.2	4.9	41.2	4.4	41.8	3.5	33.6

202
 203 While there were large discrepancies between the observed and simulated annual number of
 204 CAO days (MAE), the spatial distribution of the simulated trends matched the observed trends
 205 relatively well (Figure 2). Each model shows the largest decreases in annual CAO days across
 206 Northern Hemispheric landmasses. The MPI had the smallest historical trends because the
 207 simulation produced too few CAOs early in the historical period and too many late in the period
 208 for most places. On the other hand, the MRI has a large negative trend because it produced too
 209 many CAOs in the Arctic and western Eurasia early in the historical period. Similar to the
 210 observed trends from the ERA5, both the MPI and CESM2 had a neutral to positive trend in CAO
 211 days in Eurasia. However, the MPI more accurately replicated the location of this positive trend
 212 than the CESM2. Like the ERA5, very few simulated trends in the SH were statistically
 213 significant, though the MRI and CanESM5 most accurately simulated the positive trend in CAOs
 214 across parts of the Southern Ocean.



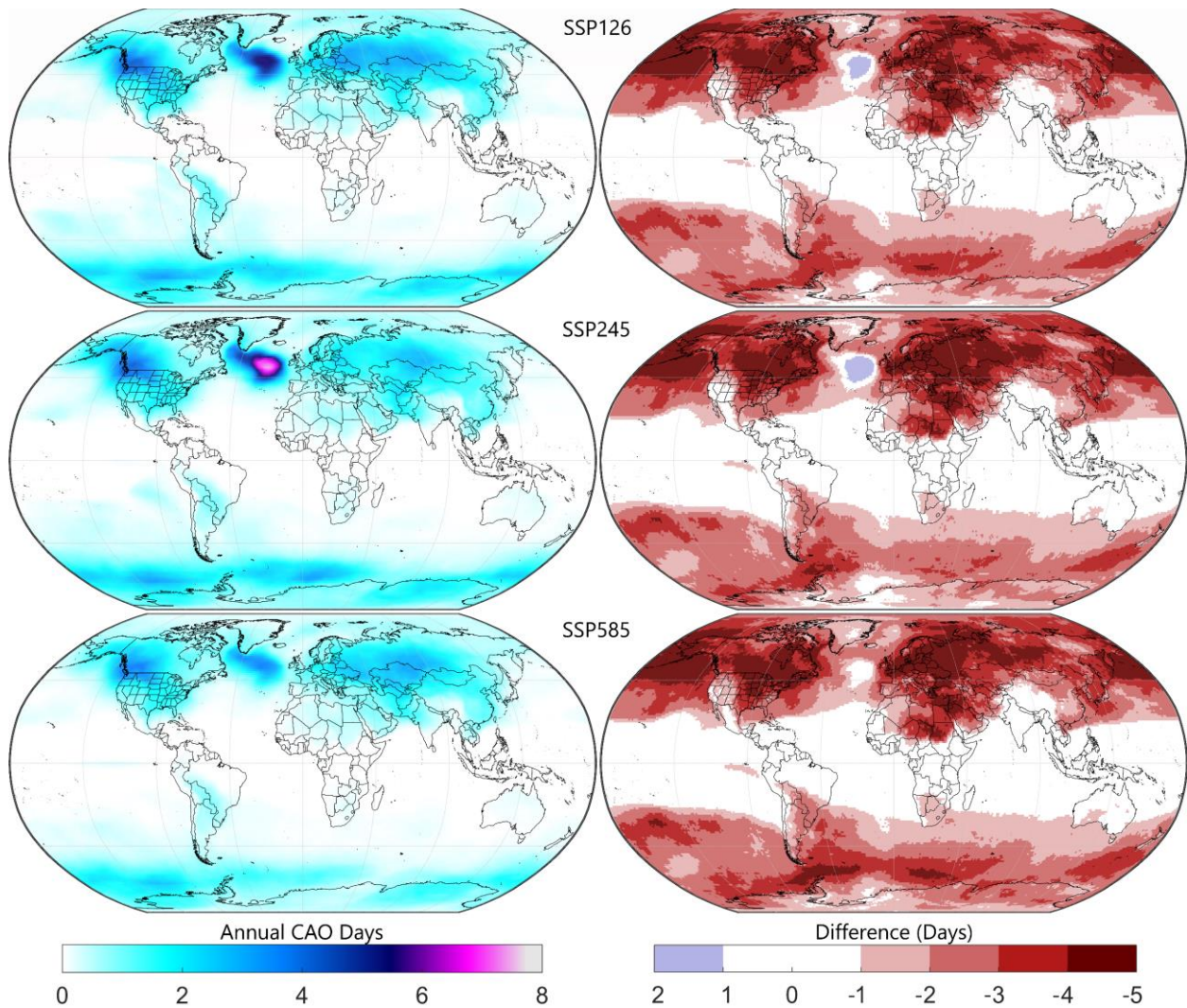
216

217 *Figure 2: Change in the mean annual number of CAO days. For the observed trends (ERA5), every 5th significant grid point at the*
 218 *$\alpha = 0.05$ level is denoted with green dots. Size and spacing of Ensemble green dots are altered because of the number of dots.*

219

220 **3.2. Future Projections of CAOs**

221 Similar to (Vavrus et al., 2006), CAOs are expected to continue decreasing across most of the
 222 globe over the next few decades. Compared to the historical period, the ensemble of each SSP
 223 shows the mean annual number of CAO days between 2015 and 2054 will decrease between
 224 50% and 100% in most locations (Figure 3). The largest decrease in annual CAO days is in North



226

227 *Figure 3: Left - ensemble of simulated annual CAO days from 2015 – 2054 for three future scenarios: SSP126, SSP245 and*
 228 *SSP585. Right - difference between each SSP and the mean annual number of CAO days from 1979 – 2014.*

229 America and Europe where CAOs have historically occurred most frequently. The CESM2,
 230 WACCM, and MRI show a large increase in CAOs across the North Atlantic, consistent with
 231 previous studies that have shown a continued weakening of the AMOC in climate model
 232 projections (Figure A2; Meehl et al., 2020; Zhang et al., 2019). The MPI and MRI also maintain a
 233 relatively large number of mean annual CAO days across North America in all three SSPs. While
 234 there are generally fewer annual CAO days with SSP245 and SSP585 than in SSP126, SSP245 and
 235 SSP585 do not necessarily result in a larger systematic decrease in CAOs. In the MPI model,
 236 more CAOs occur in the Southern Atlantic with SSP245 than SSP126. In the CESM2 model, more

237 CAOs occur in the North Atlantic (R4) from SSP245 than SSP126. SSP585 in the MPI, WACCM,
238 and CESM2 also favor more CAOs in Eurasia (R5 and R6) than in SSP245. Moreover, the WACCM
239 SSP245 simulation shows more CAOs in South America (R9) under than the SSP126 simulation.

240
241 Climate models simulate the spatial distribution and trends of CAOs well but are unable to
242 accurately model interannual variability. Though a perfect match is not expected, the large
243 discrepancies between historically simulated and observed annual CAO days indicate the
244 models may be simulating the correct trends for the wrong reasons (Luca et al., 2020). These
245 inaccurate representations of historical climate variability in the models can exacerbate errors
246 in future projections of CAOs (Maraun, 2016). As shown with the historical simulations, an
247 ensemble can be used to reduce the magnitude of individual model error, thus an ensemble is
248 also used for each SSP to better estimate changes in CAOs in each region between 2015 and
249 2054 (Figure 4).

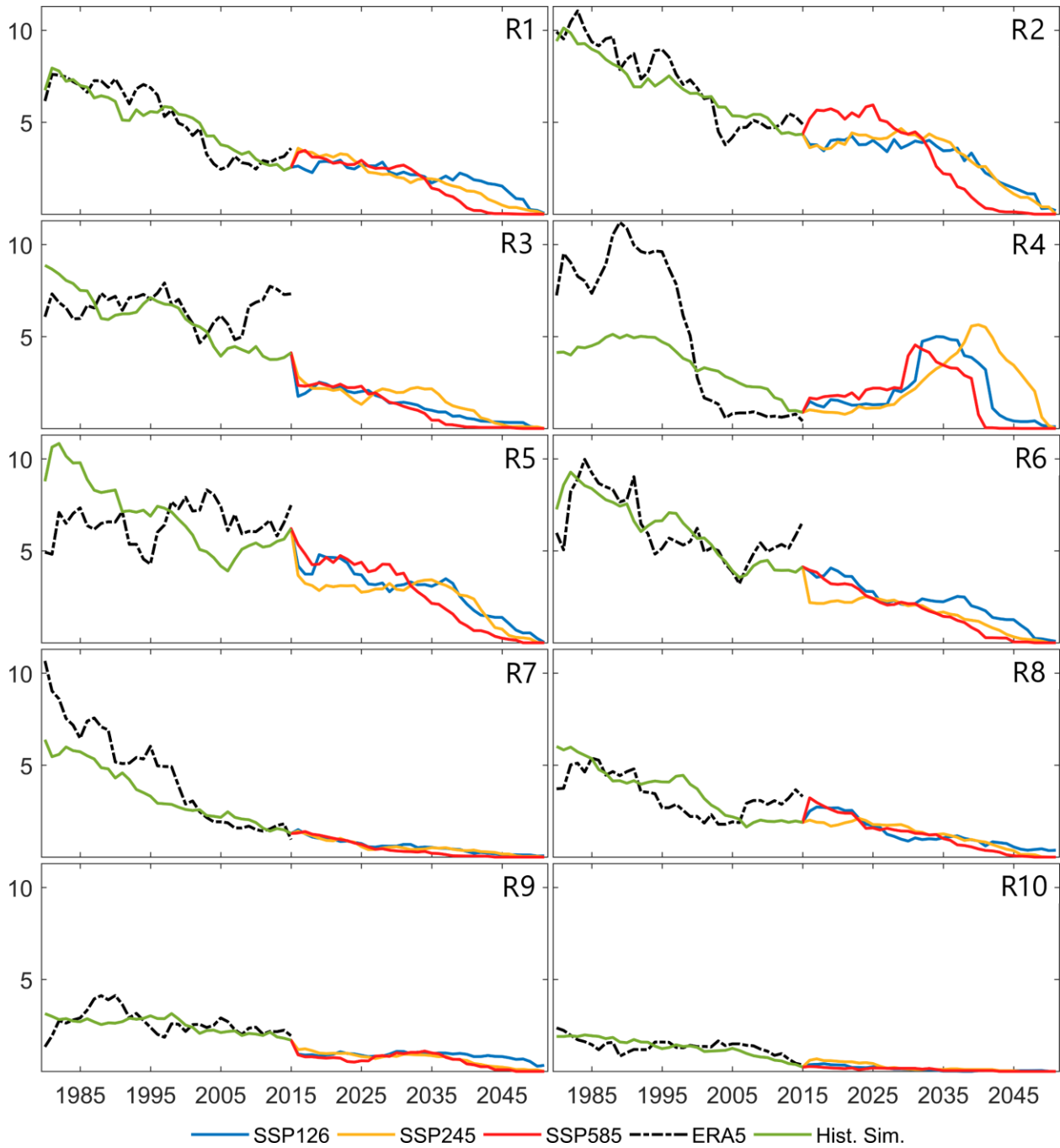
250
251 When compared with the observed annual number of CAO days for each region, the ensemble
252 matches the annual variations and trends well (Figure 4). Only R4 and R5 have particularly poor
253 historical simulations. Climate models have been shown to underestimate variability in R4 (W.
254 M. Kim et al., 2018), which may explain why historical simulations simulated too few CAOs early
255 in the historical period. The complex interaction between and amplified Arctic and surface
256 temperatures in Siberia, which is poorly represented in climate models, may account for much
257 of the discrepancy between annual CAO days simulated in R5 (Cohen et al., 2018; Labe et al.,
258 2020).

259
260 Future simulations show a consistent decrease in annual CAO days for most regions with
261 several exceptions. All three SSPs simulate a large increase in annual CAO days between 2030
262 and 2050 in R4. Though historical simulations for R4 were poor, sea ice melt and a weakening
263 of the AMOC supports the notion that the North Atlantic may be a region of large variability in
264 coming decades. In R1 and R2, future simulations show a slight increase in annual CAO days
265 through 2025 and remaining persistent through 2035 before decreasing to approximately zero

266 annual CAO days by 2054. In R3 (Alaska), historical simulations overestimate the annual number
267 of CAO days early in the historical period and underestimate the annual number of CAO days
268 late in the period which results in an overly negative trend. This suggests the models may be
269 misrepresenting variability in the North Pacific, thus the steady decline in annual CAO days in
270 R3, at least in the near-term, may be off-base. Like R3, historical simulations also
271 underestimated the number of CAO days in R6 (Europe) between 2005 and 2015. Since winter
272 extremes in Europe are heavily reliant on North Atlantic circulation (D. M. Smith et al., 2020), a
273 misrepresentation of variability in the North Atlantic may have caused the discrepancies in
274 observed and simulated CAO days in R6. In South America, annual CAO days remain consistent
275 through 2035 in all SSPs before declining to approximately zero annual CAO days in all but
276 SSP126. Across southern Africa, the already infrequent CAO days are shown to steadily decline
277 to approximately zero annual CAO days by 2035.

278

279



280

281

Figure 4: Smoothed time series of observed annual CAO days per region from the ERA5 (black), the simulated historical time series for the climate model ensemble (green) from 1979 – 2014, and the climate model ensemble projections of annual CAO days per region for each of the three SSP scenarios, SSP126 (blue), SSP245 (orange), and SSP585 (red), from 2015 - 2054.

282

283

284

285

286

287

288 **4. Conclusion**

289 CMIP6 climate models can replicate the historical spatial distribution of CAOs and capture the
290 decreasing frequency of CAOs for most of the globe. However, there are still large interannual
291 discrepancies between the historically simulated and observed number of CAO days. An
292 ensemble of historical simulations from different climate models was used to reduce errors in
293 individual models. This ensemble approach was applied to each SSP to provide the best
294 estimate of changes in CAOs for 10 regions across the globe.

295

296 Future simulations of CAOs show the decreasing frequency of CAOs in most regions will
297 continue over the coming decades and in most cases disappear by 2054, however, there are
298 several instances where CAOs increase. CAOs in the North Atlantic (R4) are shown to increase in
299 frequency between 2035 and 2050 which may be a response to the continued weakening of the
300 AMOC (Gent, 2018). The frequency of CAOs in North America and Eurasia may also remain
301 consistent over the next 10 to 20 years before decreasing to approximately zero annual CAO
302 days by 2054. In several regions, climate models incorrectly continued a decreasing trend in
303 CAOs from the historical simulation through the onset of the future simulations. This was true
304 in Europe (R6), Siberia (R5), Alaska (R3), and to a lesser extent the eastern United States (R1)
305 where the frequency of CAOs increased in the last decade. While this observed increase is not
306 likely to persist in a warming climate, the underestimated frequency of CAOs at the beginning
307 of the future simulations may have impacted the projected number of CAOs through 2054.
308 Errors in historical CAO simulations may indicate inaccuracies in future projections, thus
309 projections of CAOs in the North Atlantic and Alaska should be interpreted with caution.

310

311 Outside of the North Atlantic, all three SSPs showed the largest changes in CAO frequency to be
312 on land as opposed to the oceans. This is to be expected as the higher heat capacity of water
313 causes the oceans to change more slowly than land (Rathore et al., 2020). Though SSP126
314 generally favors a higher frequency of CAOs through 2054, SSP245 and SSP585 have a higher
315 frequency of CAOs in the near-term for several regions. This suggests interannual fluctuations in

316 CAO frequency may be more dependent on regional climate forcing than systematic warming.
317 Nonetheless, the decrease in the frequency of CAOs is evident in even the most conservative
318 scenario (SSP126) for every region.

319

320 Because this study uses the 1981 – 2010 climate normal period in the calculation of CAOs,
321 adjusting this period would certainly impact the frequency of CAOs in future simulations.
322 Though infrastructure often depends on absolute temperature thresholds, humans have been
323 shown to be negatively impacted by relative extremes (Sheridan et al., 2019). It would be
324 worthwhile for future studies to explore projected changes in the frequency of CAOs with a
325 dynamic 30-year climate normal period as opposed to a single static 30-year period.

326

327 **Acknowledgements and Data Availability**

328 The data that supports these findings are available at the Mendeley Data repository (Smith, Erik
329 (2020), “Cold Air Outbreaks”, Mendeley Data, v1. <http://dx.doi.org/10.17632/mtwfvvcvy5z.1>).
330 This repository contains a dataset with the dates of the individual CAOs as an .xlsx file. A larger
331 dataset is also available as a .mat file and requires a MATLAB license to access. These datasets
332 were created using ERA5 and CMIP6 climate model output near-surface temperature data.
333 ERA5 near-surface temperature data is available from the European Center for Medium-Range
334 Weather Forecasts (ECMWF) via the Copernicus Climate Change Service at
335 <https://cds.climate.copernicus.eu/cdsapp#!/dataset/reanalysis-era5-single-levels>. Climate
336 model output from the CMIP6 archive is publicly available from the Earth System Grid
337 Federation (ESGF; <https://esgf-node.llnl.gov/search/cmip6/>).

338 **References**

- 339 Almazroui, M., Saeed, F., Saeed, S., Nazrul Islam, M., Ismail, M., Klutse, N. A. B., & Siddiqui, M. H. (2020).
340 Projected Change in Temperature and Precipitation Over Africa from CMIP6. *Earth Systems and*
341 *Environment*, 4(3), 455–475. <https://doi.org/10.1007/s41748-020-00161-x>
- 342 Ayarzagüena, B., & Screen, J. A. (2016). Future Arctic sea ice loss reduces severity of cold air outbreaks in
343 midlatitudes: Sea Ice Loss and Midlatitude CAOs. *Geophysical Research Letters*, 43(6), 2801–
344 2809. <https://doi.org/10.1002/2016GL068092>
- 345 Bauer, N., Calvin, K., Emmerling, J., Fricko, O., Fujimori, S., Hilaire, J., Eom, J., Krey, V., Kriegler, E.,
346 Mouratiadou, I., Sytze de Boer, H., van den Berg, M., Carrara, S., Daioglou, V., Drouet, L.,
347 Edmonds, J. E., Gernaat, D., Havlik, P., Johnson, N., ... van Vuuren, D. P. (2017). Shared Socio-
348 Economic Pathways of the Energy Sector – Quantifying the Narratives. *Global Environmental*
349 *Change*, 42, 316–330. <https://doi.org/10.1016/j.gloenvcha.2016.07.006>
- 350 Bell, J. E., Brown, C. L., Conlon, K., Herring, S., Kunkel, K. E., Lawrimore, J., Luber, G., Schreck, C., Smith,
351 A., & Uejio, C. (2018). Changes in extreme events and the potential impacts on human health.
352 *Journal of the Air & Waste Management Association*, 68(4), 265–287.
353 <https://doi.org/10.1080/10962247.2017.1401017>
- 354 Cohen, J. L., Furtado, J. C., Barlow, M. A., Alexeev, V. A., & Cherry, J. E. (2012). Arctic warming, increasing
355 snow cover and widespread boreal winter cooling. *Environmental Research Letters*, 7(1),
356 014007. <https://doi.org/10.1088/1748-9326/7/1/014007>
- 357 Cohen, J., Pfeiffer, K., & Francis, J. A. (2018). Warm Arctic episodes linked with increased frequency of
358 extreme winter weather in the United States. *Nature Communications*, 9(1).
359 <https://doi.org/10.1038/s41467-018-02992-9>

360 Collins, S. N., James, R. S., Ray, P., Chen, K., Lassman, A., & Brownlee, J. (2013). Grids in Numerical
361 Weather and Climate Models. *Climate Change and Regional/Local Responses*.
362 <https://doi.org/10.5772/55922>

363 Danabasoglu, G., Lamarque, J.-F., Bacmeister, J., Bailey, D. A., DuVivier, A. K., Edwards, J., Emmons, L. K.,
364 Fasullo, J., Garcia, R., Gettelman, A., Hannay, C., Holland, M. M., Large, W. G., Lauritzen, P. H.,
365 Lawrence, D. M., Lenaerts, J. T. M., Lindsay, K., Lipscomb, W. H., Mills, M. J., ... Strand, W. G.
366 (2020). The Community Earth System Model Version 2 (CESM2). *Journal of Advances in*
367 *Modeling Earth Systems*, 12(2), e2019MS001916. <https://doi.org/10.1029/2019MS001916>

368 Davis, S. J., Lewis, N. S., Shaner, M., Aggarwal, S., Arent, D., Azevedo, I. L., Benson, S. M., Bradley, T.,
369 Brouwer, J., Chiang, Y.-M., Clack, C. T. M., Cohen, A., Doig, S., Edmonds, J., Fennell, P., Field, C.
370 B., Hannegan, B., Hodge, B.-M., Hoffert, M. I., ... Caldeira, K. (2018). Net-zero emissions energy
371 systems. *Science*, 360(6396). <https://doi.org/10.1126/science.aas9793>

372 Dee, D. P., Uppala, S. M., Simmons, A. J., Berrisford, P., Poli, P., Kobayashi, S., Andrae, U., Balmaseda, M.,
373 A., Balsamo, G., Bauer, P., Bechtold, P., Beljaars, A. C. M., van de Berg, L., Bidlot, J., Bormann, N.,
374 Delsol, C., Dragani, R., Fuentes, M., Geer, A. J., ... Vitart, F. (2011). The ERA-Interim reanalysis:
375 Configuration and performance of the data assimilation system. *Quarterly Journal of the Royal*
376 *Meteorological Society*, 137(656), 553–597. <https://doi.org/10.1002/qj.828>

377 Edwards, P. N. (2011). History of climate modeling. *WIREs Climate Change*, 2(1), 128–139.
378 <https://doi.org/10.1002/wcc.95>

379 Ehret, U., Zehe, E., Wulfmeyer, V., Warrach-Sagi, K., & Liebert, J. (2012). HESS Opinions. *Hydrology and*
380 *Earth System Sciences Discussions*, 9, 5355–5387. <https://doi.org/10.5194/hessd-9-5355-2012>

381 Eyring, V., Bony, S., Meehl, G. A., Senior, C. A., Stevens, B., Stouffer, R. J., & Taylor, K. E. (2016). Overview
382 of the Coupled Model Intercomparison Project Phase 6 (CMIP6) experimental design and

383 organization. *Geoscientific Model Development*, 9(5), 1937–1958. <https://doi.org/10.5194/gmd->
384 9-1937-2016

385 Flato, G. M. (2011). Earth system models: An overview. *WIREs Climate Change*, 2(6), 783–800.
386 <https://doi.org/10.1002/wcc.148>

387 Friedrich, T., Timmermann, A., Tigchelaar, M., Elison Timm, O., & Ganopolski, A. (2016). Nonlinear
388 climate sensitivity and its implications for future greenhouse warming. *Science Advances*, 2(11),
389 e1501923. <https://doi.org/10.1126/sciadv.1501923>

390 Gent, P. R. (2018). A commentary on the Atlantic meridional overturning circulation stability in climate
391 models. *Ocean Modelling*, 122, 57–66. <https://doi.org/10.1016/j.ocemod.2017.12.006>

392 Gutjahr, O., Putrasahan, D., Lohmann, K., Jungclaus, J. H., von Storch, J.-S., Brüggemann, N., Haak, H., &
393 Stössel, A. (2019). Max Planck Institute Earth System Model (MPI-ESM1.2) for the High-
394 Resolution Model Intercomparison Project (HighResMIP). *Geoscientific Model Development*,
395 12(7), 3241–3281. <https://doi.org/10.5194/gmd-12-3241-2019>

396 Hu, A., Meehl, G. A., Han, W., Yin, J., Wu, B., & Kimoto, M. (2013). Influence of Continental Ice Retreat
397 on Future Global Climate. *Journal of Climate*, 26(10), 3087–3111. <https://doi.org/10.1175/JCLI->
398 D-12-00102.1

399 Jeuken, A. B. M., Siegmund, P. C., Heijboer, L. C., Feichter, J., & Bengtsson, L. (1996). On the potential of
400 assimilating meteorological analyses in a global climate model for the purpose of model
401 validation. *Journal of Geophysical Research: Atmospheres*, 101(D12), 16939–16950.
402 <https://doi.org/10.1029/96JD01218>

403 Jones, G. S., Stott, P. A., & Christidis, N. (2013). Attribution of observed historical near-surface
404 temperature variations to anthropogenic and natural causes using CMIP5 simulations. *Journal of*
405 *Geophysical Research: Atmospheres*, 118(10), 4001–4024. <https://doi.org/10.1002/jgrd.50239>

406 Kalnay, E. (2003). *Atmospheric Modeling, Data Assimilation and Predictability*. Cambridge University
407 Press.

408 Kim, W. M., Yeager, S., Chang, P., & Danabasoglu, G. (2018). Low-Frequency North Atlantic Climate
409 Variability in the Community Earth System Model Large Ensemble. *Journal of Climate*, *31*(2),
410 787–813. <https://doi.org/10.1175/JCLI-D-17-0193.1>

411 Kim, Y., & Lee, S. (2019). Trends of extreme cold events in the central regions of Korea and their
412 influence on the heating energy demand. *Weather and Climate Extremes*, *24*, 100199.
413 <https://doi.org/10.1016/j.wace.2019.100199>

414 Klinger, C., Landeg, O., & Murray, V. (2014). Power Outages, Extreme Events and Health: A Systematic
415 Review of the Literature from 2011-2012. *PLoS Currents*, *6*.
416 <https://doi.org/10.1371/currents.dis.04eb1dc5e73dd1377e05a10e9edde673>

417 Kolstad, E. W., & Bracegirdle, T. J. (2008). Marine cold-air outbreaks in the future: An assessment of IPCC
418 AR4 model results for the Northern Hemisphere. *Climate Dynamics*, *30*(7), 871–885.
419 <https://doi.org/10.1007/s00382-007-0331-0>

420 Kumar, S., Merwade, V., Kinter, J. L., & Niyogi, D. (2013). Evaluation of Temperature and Precipitation
421 Trends and Long-Term Persistence in CMIP5 Twentieth-Century Climate Simulations. *Journal of*
422 *Climate*, *26*(12), 4168–4185. <https://doi.org/10.1175/JCLI-D-12-00259.1>

423 Labe, Z., Peings, Y., & Magnusdottir, G. (2020). Warm Arctic, Cold Siberia Pattern: Role of Full Arctic
424 Amplification Versus Sea Ice Loss Alone. *Geophysical Research Letters*, *47*(17), e2020GL088583.
425 <https://doi.org/10.1029/2020GL088583>

426 Lesk, C., Rowhani, P., & Ramankutty, N. (2016). Influence of extreme weather disasters on global crop
427 production. *Nature*, *529*(7584), 84–87. <https://doi.org/10.1038/nature16467>

428 Liu, Han-Li, Bardeen, C. G., Foster, B. T., Lauritzen, P., Liu, J., Lu, G., Marsh, D. R., Maute, A., McInerney, J.
429 M., Pedatella, N. M., Qian, L., Richmond, A. D., Roble, R. G., Solomon, S. C., Vitt, F. M., & Wang,

430 W. (2018). Development and Validation of the Whole Atmosphere Community Climate Model
431 With Thermosphere and Ionosphere Extension (WACCM-X 2.0). *Journal of Advances in Modeling*
432 *Earth Systems*, 10(2), 381–402. <https://doi.org/10.1002/2017MS001232>

433 Liu, H.-L., Foster, B. T., Hagan, M. E., McInerney, J. M., Maute, A., Qian, L., Richmond, A. D., Roble, R. G.,
434 Solomon, S. C., Garcia, R. R., Kinnison, D., Marsh, D. R., Smith, A. K., Richter, J., Sassi, F., &
435 Oberheide, J. (2010). Thermosphere extension of the Whole Atmosphere Community Climate
436 Model. *Journal of Geophysical Research: Space Physics*, 115(A12).
437 <https://doi.org/10.1029/2010JA015586>

438 Liu, X., Shen, B., Price, L., Hasanbeigi, A., Lu, H., Yu, C., & Fu, G. (2019). A review of international
439 practices for energy efficiency and carbon emissions reduction and lessons learned for China.
440 *WIREs Energy and Environment*, 8(5), e342. <https://doi.org/10.1002/wene.342>

441 Luca, A. D., Pitman, A. J., & de Elía, R. (2020). Decomposing Temperature Extremes Errors in CMIP5 and
442 CMIP6 Models. *Geophysical Research Letters*, 47(14), e2020GL088031.
443 <https://doi.org/10.1029/2020GL088031>

444 Maraun, D. (2016). Bias Correcting Climate Change Simulations—A Critical Review. *Current Climate*
445 *Change Reports*, 2(4), 211–220. <https://doi.org/10.1007/s40641-016-0050-x>

446 Meehl, G. A., Arblaster, J. M., Bates, S., Richter, J. H., Tebaldi, C., Gettelman, A., Medeiros, B.,
447 Bacmeister, J., DeRepentigny, P., Rosenbloom, N., Shields, C., Hu, A., Teng, H., Mills, M. J., &
448 Strand, G. (2020). Characteristics of Future Warmer Base States in CESM2. *Earth and Space*
449 *Science*, 7(9), e2020EA001296. <https://doi.org/10.1029/2020EA001296>

450 O’Neill, B. C., Kriegler, E., Riahi, K., Ebi, K. L., Hallegatte, S., Carter, T. R., Mathur, R., & van Vuuren, D. P.
451 (2014). A new scenario framework for climate change research: The concept of shared
452 socioeconomic pathways. *Climatic Change*, 122(3), 387–400. [https://doi.org/10.1007/s10584-](https://doi.org/10.1007/s10584-013-0905-2)
453 [013-0905-2](https://doi.org/10.1007/s10584-013-0905-2)

454 O'Neill, B. C., Tebaldi, C., Van Vuuren, D. P., Eyring, V., Friedlingstein, P., Hurtt, G., Knutti, R., Kriegler, E.,
455 Lamarque, J. F., Lowe, J., Meehl, G. A., Moss, R., Riahi, K., & Sanderson, B. M. (2016). *The*
456 *Scenario Model Intercomparison Project (ScenarioMIP) for CMIP6*. [https://doi.org/10.5194/gmd-](https://doi.org/10.5194/gmd-9-3461-2016)
457 [9-3461-2016](https://doi.org/10.5194/gmd-9-3461-2016)

458 Polkova, I., Köhl, A., & Stammer, D. (2019). Climate-mode initialization for decadal climate predictions.
459 *Climate Dynamics*, *53*(11), 7097–7111. <https://doi.org/10.1007/s00382-019-04975-y>

460 Raäisaänen, J. (2007). How reliable are climate models? *Tellus A: Dynamic Meteorology and*
461 *Oceanography*, *59*(1), 2–29. <https://doi.org/10.1111/j.1600-0870.2006.00211.x>

462 Randall, D. A., Wood, R. A., Bony, S., Colman, R., Fichet, T., Fyfe, J., Kattsov, V., Pitman, A., Shukla, J.,
463 Srinivasan, J., Stouffer, R. J., Sumi, A., Taylor, K. E., AchutaRao, K., Allan, R., Berger, A., Blatter,
464 H., Bonfils, C., Boone, A., ... McAvaney, B. (n.d.). *Climate Models and Their Evaluation*. 74.

465 Rathore, S., Bindoff, N. L., Phillips, H. E., & Feng, M. (2020). Recent hemispheric asymmetry in global
466 ocean warming induced by climate change and internal variability. *Nature Communications*,
467 *11*(1), 2008. <https://doi.org/10.1038/s41467-020-15754-3>

468 Richardson, L. F. (2007). *Weather Prediction by Numerical Process*. Cambridge University Press.

469 Schewe, J., Gosling, S. N., Reyer, C., Zhao, F., Ciais, P., Elliott, J., Francois, L., Huber, V., Lotze, H. K.,
470 Seneviratne, S. I., van Vliet, M. T. H., Vautard, R., Wada, Y., Breuer, L., Büchner, M., Carozza, D.
471 A., Chang, J., Coll, M., Deryng, D., ... Warszawski, L. (2019). State-of-the-art global models
472 underestimate impacts from climate extremes. *Nature Communications*, *10*(1), 1005.
473 <https://doi.org/10.1038/s41467-019-08745-6>

474 Sheridan, S. C., Lee, C. C., & Allen, M. J. (2019). The Mortality Response to Absolute and Relative
475 Temperature Extremes. *International Journal of Environmental Research and Public Health*,
476 *16*(9), 1493. <https://doi.org/10.3390/ijerph16091493>

477 Smith, D. M., Scaife, A. A., Eade, R., Athanasiadis, P., Bellucci, A., Bethke, I., Bilbao, R., Borchert, L. F.,
478 Caron, L.-P., Counillon, F., Danabasoglu, G., Delworth, T., Doblas-Reyes, F. J., Dunstone, N. J.,
479 Estella-Perez, V., Flavoni, S., Hermanson, L., Keenlyside, N., Kharin, V., ... Zhang, L. (2020). North
480 Atlantic climate far more predictable than models imply. *Nature*, *583*(7818), 796–800.
481 <https://doi.org/10.1038/s41586-020-2525-0>

482 Smith, E. T., & Sheridan, S. C. (2019). The influence of extreme cold events on mortality in the United
483 States. *Science of The Total Environment*, *647*, 342–351.
484 <https://doi.org/10.1016/j.scitotenv.2018.07.466>

485 Smith, E. T., & Sheridan, S. C. (2020). Where Do Cold Air Outbreaks Occur, and How Have They Changed
486 Over Time? *Geophysical Research Letters*, *47*(13), e2020GL086983.
487 <https://doi.org/10.1029/2020GL086983>

488 Smith, E.T. (2020), "Cold Air Outbreaks", Mendeley Data, V1, doi: 10.17632/mtwfvvcvy5z.1

489 Swart, N. C., Cole, J. N. S., Kharin, V. V., Lazare, M., Scinocca, J. F., Gillett, N. P., Anstey, J., Arora, V.,
490 Christian, J. R., Hanna, S., Jiao, Y., Lee, W. G., Majaess, F., Saenko, O. A., Seiler, C., Seinen, C.,
491 Shao, A., Sigmond, M., Solheim, L., ... Winter, B. (2019). The Canadian Earth System Model
492 version 5 (CanESM5.0.3). *Geoscientific Model Development*, *12*(11), 4823–4873.
493 <https://doi.org/10.5194/gmd-12-4823-2019>

494 Tebaldi, C., Debeire, K., Eyring, V., Fischer, E., Fyfe, J., Friedlingstein, P., Knutti, R., Lowe, J., O'Neill, B.,
495 Sanderson, B., van Vuuren, D., Riahi, K., Meinshausen, M., Nicholls, Z., Hurtt, G., Kriegler, E.,
496 Lamarque, J.-F., Meehl, G., Moss, R., ... Ziehn, T. (2020). Climate model projections from the
497 Scenario Model Intercomparison Project (ScenarioMIP) of CMIP6. *Earth System Dynamics*
498 *Discussions*, 1–50. <https://doi.org/10.5194/esd-2020-68>

499 Tokarska, K. B., Stolpe, M. B., Sippel, S., Fischer, E. M., Smith, C. J., Lehner, F., & Knutti, R. (2020). Past
500 warming trend constrains future warming in CMIP6 models. *Science Advances*, *6*(12), eaaz9549.
501 <https://doi.org/10.1126/sciadv.aaz9549>

502 Vavrus, S., Walsh, J. E., Chapman, W. L., & Portis, D. (2006). The behavior of extreme cold air outbreaks
503 under greenhouse warming. *International Journal of Climatology*, *26*(9), 1133–1147.
504 <https://doi.org/10.1002/joc.1301>

505 Wang, T., Hamann, A., Spittlehouse, D., & Carroll, C. (2016). Locally Downscaled and Spatially
506 Customizable Climate Data for Historical and Future Periods for North America. *PLOS ONE*,
507 *11*(6), e0156720. <https://doi.org/10.1371/journal.pone.0156720>

508 Wilks, D. S. (2016). “The Stippling Shows Statistically Significant Grid Points”: How Research Results are
509 Routinely Overstated and Overinterpreted, and What to Do about It. *Bulletin of the American*
510 *Meteorological Society*, *97*(12), 2263–2273. <https://doi.org/10.1175/BAMS-D-15-00267.1>

511 Yukimoto, S., Kawai, H., Koshiro, T., Oshima, N., Yoshida, K., Urakawa, S., Tsujino, H., Deushi, M., Tanaka,
512 T., Hosaka, M., Yabu, S., Yoshimura, H., Shindo, E., Mizuta, R., Obata, A., Adachi, Y., & Ishii, M.
513 (2019). The Meteorological Research Institute Earth System Model Version 2.0, MRI-ESM2.0:
514 Description and Basic Evaluation of the Physical Component. *Journal of the Meteorological*
515 *Society of Japan. Ser. II*, *97*(5), 931–965. <https://doi.org/10.2151/jmsj.2019-051>

516 Yun, W.-T., Stefanova, L., & Krishnamurti, T. (2003). Improvement of the Multimodel Superensemble
517 Technique for Seasonal Forecasts. *Journal of Climate*, *16*, 3834–3840.
518 [https://doi.org/10.1175/1520-0442\(2003\)016<3834:IOTMST>2.0.CO;2](https://doi.org/10.1175/1520-0442(2003)016<3834:IOTMST>2.0.CO;2)

519 Zahn, M., & von Storch, H. (2010). Decreased frequency of North Atlantic polar lows associated with
520 future climate warming. *Nature*, *467*(7313), 309–312. <https://doi.org/10.1038/nature09388>

521 Zhang, R., Sutton, R., Danabasoglu, G., Kwon, Y.-O., Marsh, R., Yeager, S. G., Amrhein, D. E., & Little, C.
522 M. (2019). A Review of the Role of the Atlantic Meridional Overturning Circulation in Atlantic

523 Multidecadal Variability and Associated Climate Impacts. *Reviews of Geophysics*, 57(2), 316–375.

524 <https://doi.org/10.1029/2019RG000644>

525

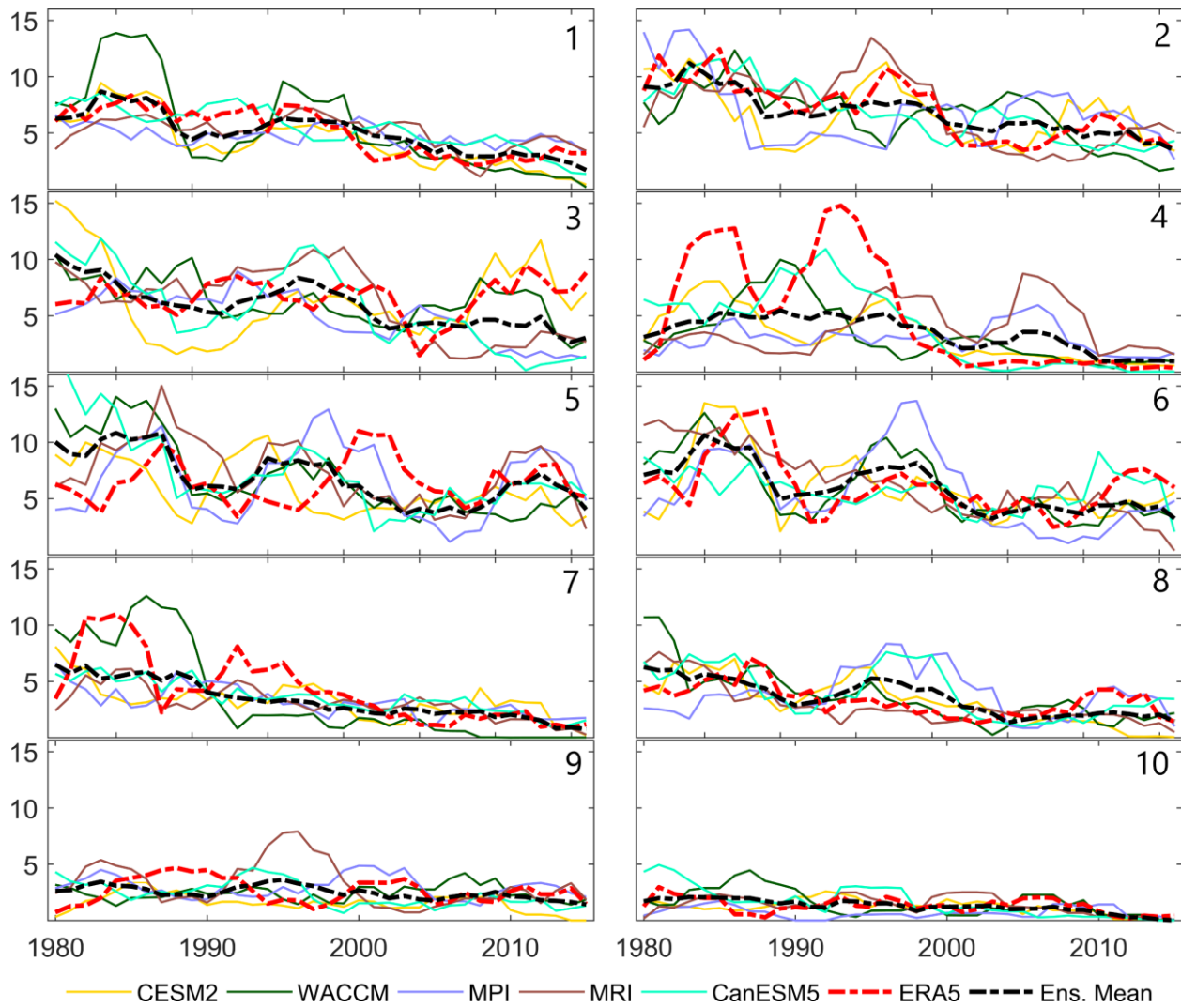
526 **Appendix**

527

528 *Table A2: Information for the CMIP6 models used in this study.*

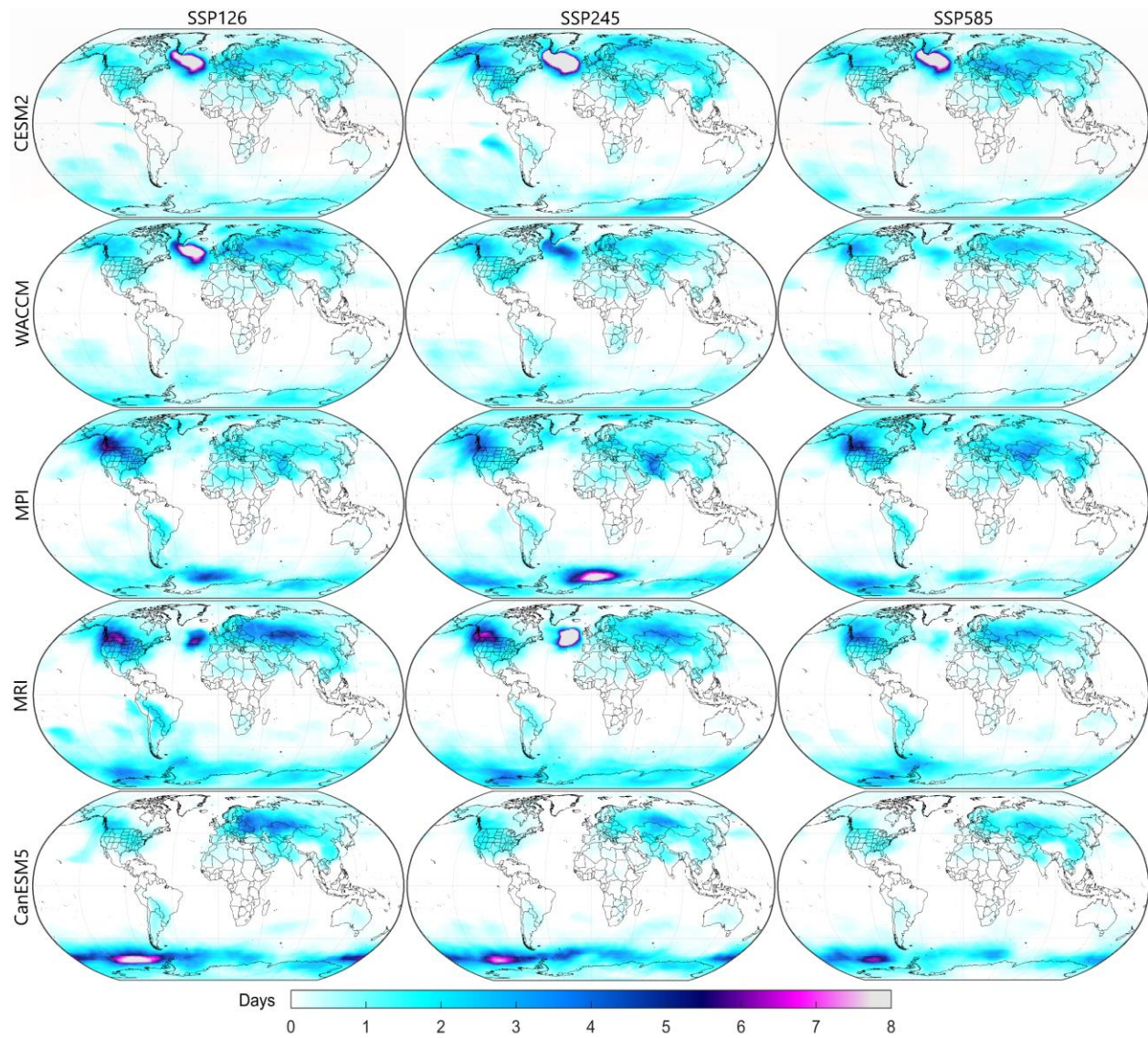
Model	Native Resolution	Country	Variant	Reference
CESM2	1.3° × 0.9°	USA	r1i1p1f1	Danabasoglu et al. (2020)
CESM2-WACCM	1.3° × 0.9°	USA	r1i1p1f1	Danabasoglu et al. (2020)
MPI-ESM1-2-HR	0.9° × 0.9°	Germany	r1i1p1f1	Gutjahr et al. (2019)
MRI-ESM2-0	1.1° × 1.1°	Japan	r1i1p1f1	Yukimoto et al. (2019)
CanESM5	2.8° × 2.8°	Canada	r1i1p1f1	Swart et al. (2019)

529



531 *Figure A1: Annual number of CAO days (y-axis) simulated by each climate model (solid lines), observed with ERA5 (red dashed*
 532 *line), and the climate model mean (black dashed line) from 1979 – 2015 (x-axis). Regions are denoted by the numbers in the top*
 533 *right corner. Lines are smoothed using a 5-year centered moving average.*

534



535

536 *Figure A2: Simulated annual CAO days from 2015 – 2054 for three future scenarios: SSP126, SSP245 and SSP585 for each of the*
 537 *five climate models.*

538